Coupled nature of magnetic and structural transition in MnNiGe under pressure

S. Anzai
Faculty of Engineering, Keio University, Hiyoshi, Yokohama-shi, 223, Japan

K. Ozawa
Solid State Physics Laboratory, Japan Atomic Energy Research Institute, Tokai-mura, Ibaraki, 319-11, Japan
(Received 9 January 1978)

Differential-thermal-analysis investigation in MnNiGe under pressure (<8 kbar) shows that (i) the first-order TiNiSi-to-Ni_2In-type structural transition point T_D decreases with increasing hydrostatic pressure ($dT_D^b/dP = -12.2$ and $dT_D^c/dP = -10.0$ K/kbar); (ii) the second-order helimagnetic-to-paramagnetic transition point T_N situated below T_D, increases with pressure ($dT_N/dP = +2.3$ K/kbar); (iii) T_N and T_D coincide to draw a new first-order transition line $T_{COL}(P)$ above a triple point $P_{TRI} = 3$–4 kbar and that the pressure slope ($dT_{COL}^b/dP = dT_{COL}^c/dP = -5.4$ K/kbar) is intermediate in value between those for T_D and T_N. This is the first example of a collaborating phase transition in which two distinctly different physical properties can cause either a simultaneous transition or two separate ones. A simple phenomenological theory, based upon a Landau-like free-energy expression, provides an understanding of the collaborating magnetic and structural transition in MnNiGe. A mechanism for this transition is proposed.

I. INTRODUCTION

By introducing cross terms between the basic axial components of polarization in the power-series expression for the free energy, Devonshire[1] gave a phenomenological explanation of the ferroelectric-to-paraelectric transition through several distinct ferroelectric states. Thereafter, many intricate features of solid-solid transitions in the various types of physical systems have been understood by means of coupled order parameters. All the examples may be classified according to the physical origins of the coupled order parameters. (a) The coupled order parameters are chosen to be variations of the same kind of physical origins, e.g., the aforementioned anisotropic polarizations, anisotropic magnetizations in weak ferromagnets,[2] anisotropic exchange interactions yielding a tetracritical point,[3,4] and two real amplitudes of distortions in the commensurate-incommensurate phase transition of charge-density-wave (CDW) systems.[5] Cross terms involving interactions between different kinds of physical properties are identified as cases (b) and (c). (b) The transition occurs for both order parameters simultaneously, but its driving force is contained in only one of them. The other one can only change with the former in a cooperative sense. One such example is the exchange striction effect[6] in which the magnetic order parameter and the deviation in atomic distance from the normal thermal-expansion behavior correspond to the former and latter cases, respectively. No finite value exists for the latter when the former has zero value. (c) Respective parameters drive the separate kinds of transitions and can also coherently drive a simultaneous transition under suitable conditions. We call this last type (c) a collaborating transition between different kinds of physical properties.

As the examples of the (c)-type transition, we have Smolenskii's formulation[7] in which the ordering of spins and electric dipoles occurs simultaneously as a result of ionic displacement. Huberman and Streifer[8] have developed the free-energy expression for the coupled order parameters between lattice disorder (atomic displacements towards interstitial sites) and magnetic order-disorder transitions, and drawn a relationship among the lattice ordered ferromagnetic and paramagnetic, and the lattice disordered paramagnetic phases. MnBi exemplified by them exhibits only a simultaneous transition between the lattice ordered (NiAs-type) ferromagnetic and the lattice disordered (Ni_2In-type) paramagnetic phase; separate transitions in magnetic and lattice systems in MnBi have not been reported. Although many examples have been extensively investigated for cases (a) and (b), little experimental work has been reported for type (c).

Recent neutron-diffraction studies by Bazela *et al.*[9] have disclosed that the orthorhombic, TiNiSi-type ($Pnma$) MnNiGe exhibits a helimagnetic-to-paramagnetic transition with the transition temperature $T_N = 346$ K. The magnetic moments are localized only on Mn atoms and the helical propagation vector runs along the a axis with $\tau = 0.24$–0.26. A first-order structural transition to the hexagonal, Ni_2In-type ($P6_3/mmc$) occurs at a transition temperature T_D in the paramagnetic region.[9,10] It is also reported that the Ni_2In-type $Mn_{0.9}Ni_{0.9}Ge$ has a magnetic order-disorder transition point at $T_N^{\dagger} = 273$ K.[11] These behaviors

indicate that, in the Mn-Ni-Ge system, the spin and the lattice systems can independently cause the magnetic and the structural transitions, respectively. Furthermore, the large difference in the magnetic transition temperatures between the Ni_2In- and the TiNiSi-type phases implies possibility of coherent coupling between the spin and the lattice systems in the TiNiSi-type MnNiGe.

A negative volume change (1.6%) at T_D has been found in the thermal expansivity,[9] while one can see only feeble changes in volume or in its temperature slope at T_N. From the negative sign of dT_D/dP estimated from the Clausius-Clapeyron relation, we expect that the magnetic and the structural transition lines will intersect at a point on the P-T diagram. The present paper describes the experimental results of pressure effects on T_D and T_N (Sec. III). A picture for the collaborating magnetic and structural transitions in MnNiGe is proposed in Sec. IV, based on the crystallographic and energetic considerations.

II. EXPERIMENTAL METHOD

Powders of Mn (99.99% pure), Ni (99.99% pure), and Ge (99.9999% pure) were mixed in equiatomic proportion, and packed in a mullite crucible. The mixture, sealed in a silica tube, was melted at 1200 °C, and homogenized at 800 °C for 3 days. Finally, it was cooled quickly from 300 °C. The x-ray powder pattern was indexed as the TiNiSi-type structure, although traces of impurity lines were present. The orthorhombic lattice parameters were determined to be $a = 6.022 \pm 0.016$ Å, $b = 3.747 \pm 0.004$ Å, and $c = 7.065 \pm 0.010$ Å at 300 K with Si as a standard. The resistivity of a disk, formed under pressure, was found to be 1×10^{-2} Ω cm at 300 K.

The structural and the magnetic transition temperatures were measured by following the differential-thermal-analysis (DTA) peaks[10] at hydrostatic pressures up to 8 kbars. Thermocouples were inserted both in the sample and the reference material (Al_2O_3 powder). A large working volume, 40-mm $D \times 170$-mm L, is available in the pressure vessel, which can be heated internally. The pressure system used has been described previously.[12]

III. EXPERIMENTAL RESULTS

Figure 1 shows the representative isobaric DTA patterns taken on heating and cooling at rates of about 5 K/min and at the indicated pressures. The valley and the peak temperatures recorded at ambient pressure (curves A and C) are in reasonable agreement. They are close to the peak temperature on the χ-T curve shown in the inset, where the peak temperature of χ has been assigned

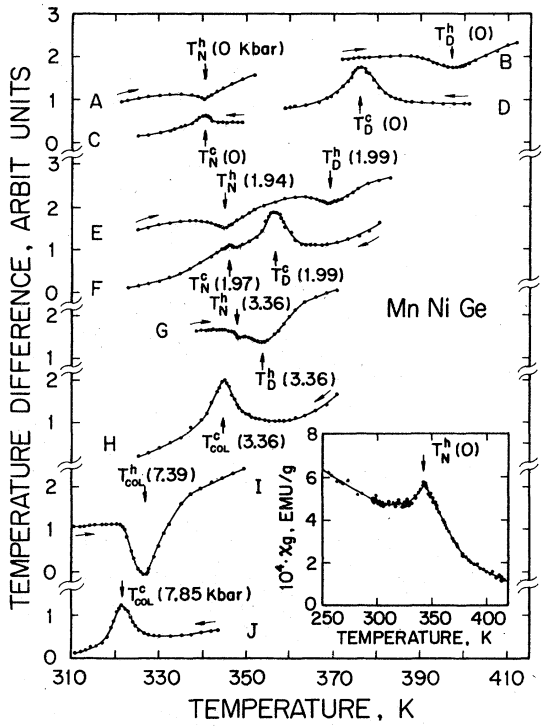

FIG. 1. Representative isobaric DTA patterns in MnNiGe. The numerical values in parentheses represent the pressure in kbars. The inset shown the temperature dependence of magnetic susceptibility χ at 7.5 koe.

as the helimagnetic-to-paramagnetic transition point in the neutron diffraction study[9]; this transition is of second order. As seen on curves B and D, a remarkable hysteresis interval of temperature between T_D^h and T_D^c is determined to be about 20 K with no detectable variation for different heating and cooling rates between 2 and 25 K/min. Here, the superscripts h and c refer to data taken in heating and cooling runs, respectively. Curves E, F, and G show that T_N shifts to higher temperatures with increasing pressure, while T_D^h and T_D^c decrease rapidly. T_N and T_D meet at a pressure between 3 and 4 kbars. Curves H and I indicate that no transition points T_N, T_D^h, and T_D^c are observed at the temperatures which are expected on the extrapolated curves for these transition points. Curves H, I, and J show new transition points T_{COL}^h and T_{COL}^c of which hysteresis interval of temperature indicates the first-order character of this transition. The transition found above P_{TRI} is considered to be a simultaneous magnetic and structural one.

Figure 2 shows the transition temperatures as a function of pressure. The pressure slopes dT_N/dP, dT_D^h/dP, and dT_D^c/dP are determined to be +2.3, −12.2, and −10.0 K/kbar, respectively. With increasing pressure, a linear shift of T_{COL}

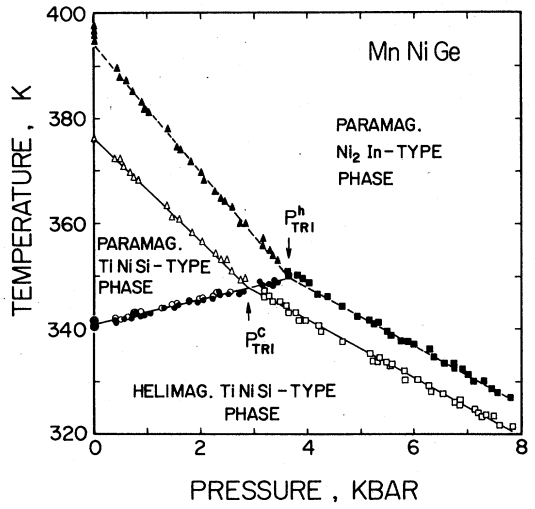

FIG. 2. P-T diagram among the helimagnetic TiNiSi-type, the paramagnetic TiNiSi-type, and the paramagnetic Ni_2 In-type phases. Closed and open symbols represent the cooling and heating runs, respectively. The triple point P_{TRI} is determined to be 3.6 kbars on heating and 2.9 kbars on cooling.

towards lower temperatures is observed with a slope of $dT^h_{COL}/dP = dT^c_{COL}/dP = -5.4$ K/kbar. A triple point P_{TRI} among $T_N(P)$, $T_D(P)$, and $T_{COL}(P)$ is found in the P-T diagram. These pressure effects on the transition lines are confirmed to be reversible with the pressure-cycled experiments.

IV. DISCUSSIONS

The structural data at 550 K (paramagnetic Ni_2In type) and 295 K (helimagnetic TiNiSi type)[9] are depicted in Figures 3(a)–3(d). The Ni_2In-type structure consists of honeycomb layers[13] of Ni and Ge atoms with the interplaner spaces filled by Mn atoms [Figs. 3(a) and 3(b)]. The atomic distance between Ni and Ge atoms is 2.38 Å, which agrees with the sum of radii[14] for Ni (1.24 Å) and Ge (1.16 Å) atoms. The nearest neighboring distances for Mn(1)-Mn(2) atoms along the c_{hex} axis is 2.76 Å, which is nearly twice as large as the atomic radius of Mn atom (1.39 Å). Here, the hexagonal lattice parameters a_{hex} and c_{hex} are related to the orthorhombic parameters in the following manner: $a = c_{hex}$, $b = a_{hex}$, and $c = \sqrt{3}a_{hex}$. The nearest-neighboring Mn-Ge and Mn-Ni distances are 2.75 Å, which are slightly larger than the sum of the respective atomic radii. It seems that the crystal structure of the Ni_2In-type MnNiGe is mainly supported by the honeycomb layers stitched up by the Mn chains along the c_{hex} axis. The next-nearest-neighboring Ni and Ge atoms form a chain along the c_{hex} axis, and are

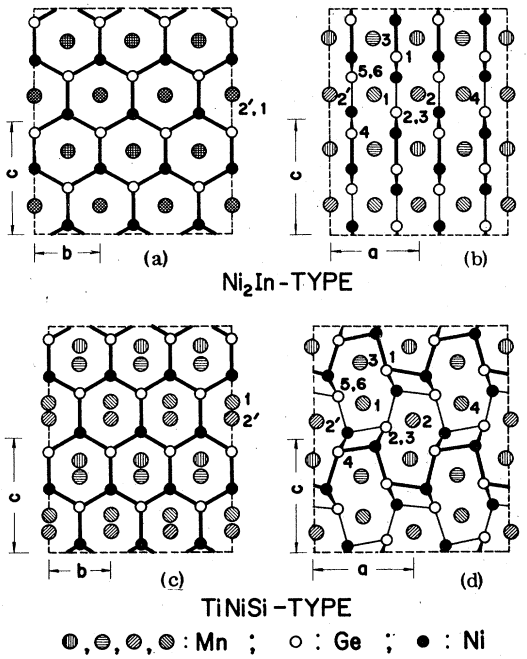

FIG. 3. Projections of the Ni_2In- and the TiNiSi-type structures on the b-c and a-c planes. Atoms connected by thick and thin lines are separated by half a translation period in the projection direction. The atomic distances in the TiNiSi-type phase are as follows: ^{d}Mn (1)-Ge (1) = 2.52 Å ($r-\Delta r$); ^{d}Mn (1)-Ge (2, 3) = 2.78 Å (r); ^{d}Mn (1)-Ge (4) = 3.50 Å ($r+3\Delta r$); ^{d}Mn (1)-Ge (5, 6) = 2.51 Å ($r-\Delta r$), where their approximate distances are expressed by r (= 2.75 Å) and Δr (= 0.25 Å) in parentheses.

weakly coupled to each other because the atomic distance (2.76 Å)[9] is larger than the sum of the atomic radii.[14]

In the TiNiSi-type structure [Figs. 3(c) and 3(d)], the atomic distances along the a axis are alternately shortened to 2.40 Å, which is close to the sum of the radii for Ge and Ni atoms. This bridge formation among the honeycomb layers stabilizes the three-dimensional network of Ni and Ge atoms. The next-nearest-neighboring Mn atoms [Mn(1) and Mn(3)] are locked into the interstitial sites of this network so that the c axis slightly decreases below T_D. Repulsive forces among these Mn atoms expand the alternate Ni-Ge distances (3.71 Å) along the a axis. Hence, the a axis expands at T_D when the sample is cooled. This axial stress is released by shrinkage along the b axis in compliance with Poisson's constant. These features are consistent with the thermal expansion behavior observed at T_D.[9]

Although no thermal vibration measurement has been carried out for MnNiGe, Jeitschko[15] has investigated the root-mean-square amplitudes of thermal displacements in the isomorphic MnCoGe, which also undergoes a structural transition to

the TiNiSi-type phase below T_D. He found considerably larger vibrational amplitudes for Co and Ge atoms along the c_{hex} axis, while those for Mn atoms are rather smaller along the other axes. Therefore, it is plausible that the locking phenomenon for Mn atoms is a secondary effect of the bridge formation. The pairwise coupled state for the bridge between Ni and Ge atoms is the ground state at lower temperatures. We note that Nebenzahl[16] has investigated a ground-state wave function, including correlations for spins coupled with a singlet state, and suggested the possibility of forming a stronger bond with one of the neighbors than with the other, through distortions in the atomic chain. The stability of the bridge formation might collapse as a result of the thermal excitation of electrons into excited states, supported by the lattice vibrations. The packing feature for the constituent atoms is more dense in the Ni_2In-type structure than in the TiNiSi-type MnNiGe. Moreover, the electron cloud on the Ge atom is considered to be easily deformed by external forces or internal stresses because its dielectric polarization constant[14] is as large as those for normal metal atoms. Depressing effects of hydrostatic pressure and of Mn deficiencies[17] on T_D are understood by this mechanism.

Although the cell volume of the Ni_2In-type phase is smaller than that of the TiNiSi type,[9] the decrease in cell volume introduced by pressure could not depress the T_N; instead, $dT_N/dP>0$ as observed below P_{TRI}. Hence, the exchange striction effect is considered to be of secondary importance in the isobaric process. Thus, we provide the following exchange interactions. The helical order indicates that the adjacent Mn spins along the helical propagation vector are coupled in the nearly ferromagnetic alignment with the effective exchange integral $J_{eff}=3J_s+J_d>0$, and that there exists a second-nearest-neighboring Mn interaction $J_2<0$ along the vector [e.g., between the Mn(1) and Mn(4) atoms]. Here, J_{eff} presumably consists of a combination of the three superexchange interactions J_s via nearest-neighboring Ge atoms and the direct exchange one J_d.

In the Ni_2In-type structure, we assume that the potential exchange integral J_d is caused by the overlapping of the nearest-neighboring Mn orbitals which are directed towards each other in the Mn chain, along the c_{hex} axis. In the cross section perpendicular to the chain axis, the absolute amplitude of the Mn wave function decreases at a rate which is nearly proportional to the increase in distance from the chain axis. As seen in Figs. 3(c) and 3(d), the Mn-atomic chain along the a axis becomes a zigzag arrangement in the TiNiSi-type structure. The overlapping portion between the Mn orbitals has the maximum value when the Mn chain runs straight, but it is orthogonally reduced with the increase of the zigzag displacement; this is related to a single deformation parameter ζ. Thus, we obtain the relationship $J_d=J_d^{\dagger}(1+\beta\zeta^2)$, which satisfies the requirement that the nondisplaced state has the maximum $|J_d|$. Here, $J_d^{\dagger}$ and $\beta=(1/J_d^{\dagger})[\partial J_d/\partial(\zeta^2)]$ are constant. J_s is proportional to $<b_{\mathrm{Mn(1)\text{-}Ge}(i)}><b_{\mathrm{Mn(2)\text{-}Ge}(j)}>$ in the kinetic exchange mechanism,[18] where the terms in angular brackets represent the averaged charge transfer integrals between the Mn atoms and their Ge environments labeled by i and j. In the Ni_2In-type phase, $J_s\propto b_r^2$ holds, where b_r is the transfer integral between the nearest-neighboring Mn and Ge atoms whose distance r is the same (2.75 Å) for all. By using a notation $\Delta r\simeq 0.25$, we can represent all the distances between a Mn atom and its Ge environments in TiNiSi-type phase. Since the c axis varies with change in magnetic order parameter below T_N, it is expected that the exchange integrals vary with changing atomic spacings in MnNiGe through the exchange striction mechanism. However, the effect of the linear change in r due to the structural transition on J_s is cancelled out, as shown in the following estimation:

$$
\begin{aligned}
<b_{\mathrm{Mn(1)\text{-}Ge}(i)}><b_{\mathrm{Mn(2)\text{-}Ge}(j)}> &= (b_r/3)^2[(1)_{\mathrm{Mn(1)\text{-}Ge(2)}}+(1)_{\mathrm{Mn(1)\text{-}Ge(3)}}+(1+\alpha\Delta r)_{\mathrm{Mn(1)\text{-}Ge(1)}}] \\
&\quad\times[(1+\alpha\Delta r)_{\mathrm{Mn(2)\text{-}Ge(2)}}+(1+\alpha\Delta r)_{\mathrm{Mn(2)\text{-}Ge(3)}}+(1-3\alpha\Delta r)_{\mathrm{Mn(2)\text{-}Ge(1)}}] \\
&= b_r^2+O((\Delta r)^2),
\end{aligned}
$$

where the coefficient α is defined as $(1/b_r)(\partial b/\partial r)$. Here, the charge-transfer integral is assumed to relate linearly to the distance between Mn and Ge atoms.

By using the well-known expression,[17] one can write the magnetic transition temperature for this system,

$$
\begin{aligned}
T_N(P) &= J_o-[3J_s(1+\omega') \\
&\quad +J_d^{\dagger}(1+\beta\zeta^2)]^2/4J_2(1+\omega'')-2J_2(1+\omega'') \\
&\equiv T_N^{\dagger}(P)(1+\beta'\zeta^2+\Omega'), \qquad (1)
\end{aligned}
$$

where the intraplaner interaction J_o is assumed to be constant on ζ for simplicity. Here, $T_N^{\dagger}(P)$ is

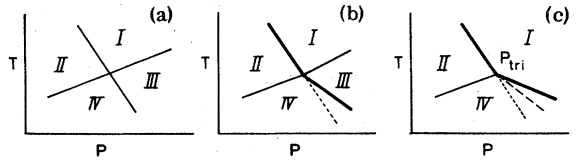

FIG. 4. Schematic representations of the P-T diagram illustrating two crossed phase-transition lines. Thick and thin lines represent the first-order and the second-order ones, respectively. Here, the phases are defined as follows. I: $\zeta=0$, $\eta=0$; II: $\zeta\neq 0$, $\eta=0$; III: $\zeta=0$, $\eta\neq 0$; and IV: $\zeta\neq 0$, $\eta\neq 0$. (a) Two second-order transition lines. (b) One first-order and one second-order transition line. The dotted line shows the extrapolated T_D line. (c) One first-order and one second-order transition line are also crossed, but B changes its sign suddenly through the structural transition line. The dashed line represents the fictitious $T_{H(T\to N)}$ line defined in (b) through Eq. (3).

the magnetic transition point when the structure is not deformed. We will discuss the physical meaning of the constants ω', ω'', and Ω'. For the free energy near P_{TRI}, we write the Landau-type[20] expression in powers of the magnetic and the deformation parameters ζ and η, respectively, as follows:

$$\Phi(T,P,\zeta,\eta)=a[T-\Theta_D(P)]\zeta^2+\epsilon\zeta^4+K\zeta^6 + b[T-T_N^{\dagger}(P) \times(1+\beta'\zeta^2+\Omega')]\eta^2+f\eta^4, \quad (2)$$

where the constants are required to have the signs ϵ (<0), K (>0), f (>0), b (>0), and a (<0). This expression[21] is the simplest form, which gives the first-order structural and the second-order magnetic transitions, separately, within the translational invariances for the free energy.

The equilibrium condition for both phases on the transition line, together with the extremum conditions for ζ and η, yields the sudden change in deformation parameter: $\zeta=(-\epsilon/2K)^{1/2}$ at $T_D=\Theta_D(P)+\epsilon^2/4Ka$ below P_{TRI}. The similar technique yields the second-order magnetic transition line

$$T_N=(2D/3Kb)[\epsilon+(\epsilon^2-3AK)^{1/2}]+T_N^{\dagger}(P)(1+\Omega').$$

Here, the abbreviations are defined as $D=(-b/2)\beta' T_N^{\dagger}(P)$, $A=a[T-\Theta_D(P)]$, and $B=b[T-T_N^{\dagger}(P)\times(1+\Omega')]$.

Above the crossing point of these magnetic and the structural transition lines, one expects a first-order structural transition line between the helimagnetic TiNiSi-type and a helimagnetic Ni_2In-type phases which are bounded by the transition line,

$$T_{H(T\to N)}=\Theta_D(P)+\epsilon^2/4aK - (D/a)[(-BK+\epsilon D)/fK] \quad (3)$$

The third term implies that this line lies above T_D when $-BK+\epsilon D>0$. This feature of the phase diagram is depicted in Fig. 4(b), together with the case [Fig. 4(a)] of two second-order phase transition lines ($K=0$), which corresponds to Liu and Fisher.[3] However, the present experimental results show no helimagnetic Ni_2In-type phase. If the parameter B becomes positive above the structural transition line, then the helimagnetic Ni_2In-type phase cannot be stabilized because no real value of η exists through the relation $\eta^2=-B/2f$. The equilibrium condition

$$\Phi_{\text{helimagnetic TiNiSi-type phase}}-\Phi_{\text{paramagnetic Ni}_2\text{In-type phase}}=A\zeta^2+\epsilon\zeta^4+K\zeta^6-(BD/f)\zeta^2-B^2/4f-(D^2/f)\zeta^4=0$$

at T_{COL} gives no zero value for ζ on the transition line. Moreover, η also jumps suddenly at this line through the relation: $\eta^2=-B/2f-D\zeta^2/f$ which is derived through the extremum condition. Then, the relation $T_D<T_{H(T\to N)}<T_{\mathrm{COL}}<T_N^F$ is derived from

$$\Phi_{\text{helimagnetic TiNiSi-type phase}}>\Phi_{\text{helimagnetic Ni}_2\text{In-type phase}}=-B^2/4f$$

in the temperature region between $T_{H(T\to N)}$ and T_N^F. Here, T_N^F is the fictitious helimagnetic-to-paramagnetic transition line of the Ni_2In-type phase. This situation is depicted in Fig. 4(c).

Such a condition would be realized in the following process. We assume J_s negative sign with $|3J_s|<J_d$ (so that $J_d>0$). J_s is maintained with the nearest-neighboring Ge atoms which are almost isolated from their nearest-neighboring Ni-Ge honeycomb layers. Hence, the transfered electrons from the Mn atoms transfer to the nearest neighboring Mn atoms through the Ge atoms. However, even an arbitrarily small displacement of the Ni and Ge atoms from their symmetrical positions in the initial Ni_2In-type phase is sufficient to produce an abrupt change in the superexchange interaction J_s. This is because the Ni-Ge pair formation along the a axis enhances the charge transfer probability between the second-nearest-neighboring Mn(1)-Mn(4) interactions J_{2s} through the pair on the Ni-Ge three-dimensional network and decreases the probability for J_s as the compensation of J_{2s}. The formation of the Ni-Ge pair undergoes a sudden change in J_s or J_{2s} at the structural transition point. The changes are expressed with the constants ω' and ω'', respectively. Provided that the decrease in $|J_s|$ overcomes the increase in $|J_{2s}|$ through this mechanism,

then $T_N(P) \gg T_N^{\dagger}(P)$ is satisfied. This constriction condition is plausible because the magnetic transition point of the Ni_2In-type $Mn_{0.9}Ni_{0.9}Ge$ is considerably lower than that of the TiNiSi-type MnNiGe. In order to express this circumstance, we used the parameter Ω' in (2), which is a positive constant in the TiNiSi-type and zero in the Ni_2In-type phases. Such a change in sign of B can be possible in case (c), because one of the transition systems has the freedom to change the other system essentially. This freedom cannot be allowed in case (a).

This is the explanation for the experimental result that the system has a total three phases rather than the four expected in the current papers[22] and T_{COL} lies above the extrapolated T_D line. Positive sign of J_d implies $\beta < 0$, which requires $\beta' < 0$. Then, T_N increases when ζ decreases with lowering T_D. This is an explanation of $dT_N/dP > 0$. By rearranging the terms in Eq. (2) in the sequence of ζ powers, one can see the square of the oscillation mode concerning to the deformation, given by $a(T-\Theta_D)$, is strengthened with the magnetic forces $-bT_N^{\dagger}(P)\beta'\eta^2$. It is considered that the stability of the deformed structure is backed up by the effective magnetic interactions which are mutually enhanced by the deformation. Such a collaborating feature is supported by the observed slope dT_{COL}/dP which lies between the values of dT_N/dP and dT_D/dP. This is a picture of the collaborating magnetic and structural transition in MnNiGe.

V. CONCLUSION

Our pressure experiments reveal the following three facts: (i) T_D and T_N decrease and increase, respectively, with increasing hydrostatic pressure; (ii) T_D and T_N coincide to a simultaneous first-order magnetic and structural transition line $T_{COL}(P)$ above a triple point P_{TRI}; and (iii) the pressure slope for T_{COL} lies between those for T_N and T_D. On the basis of crystallographic and energetic considerations, it is concluded that the structural deformation and the magnetic interactions collaborate mutually to drive a simultaneous transition between the helimagnetic TiNiSi-type and the paramagnetic Ni_2In-type phases through the coupled term between the deformation and the magnetic order parameters. This is the first clear-cut example of collaborating transitions between different kinds of physical properties.

ACKNOWLEDGMENT

The authors express their thanks to Dr. E. F. Skelton of Naval Research Laboratory for discussions.

[1] A. F. Devonshire, Adv. Phys. 3, 85 (1954).
[2] I. E. Dzialoshinskii, Zh. Eksp. Teor. Fiz. 32, 1547 (1957) [Sov. Phys.-JETP 5, 1259 (1957)].
[3] K. S. Liu and M. E. Fisher, J. Low Temp. Phys. 10, 655 (1973).
[4] A. D. Bruce and A. Aharony, Phys. Rev. B 11, 478 (1975).
[5] D. E. Moncton, J. D. Axe, and F. J. Disalvo, Phys. Rev. Lett. 34, 734 (1975).
[6] C. Kittel, Phys. Rev. 120, 335 (1960).
[7] G. A. Smolenskii, Fiz. Tverd. Tela 4, 1095 (1962) [Sov. Phys.-Solid State 4, 807 (1962)].
[8] B. A. Huberman and W. Streifer, Phys. Rev. B 12, 2741 (1975).
[9] W. Bażela, A. Szytuła, J. Todorović, Z. Tomkowicz, and A. Zięba, Phys. Status Solidi A 38, 721 (1976).
[10] V. Johnson, Inorg. Chem. 14, 1117 (1975).
[11] K. S. V. Narasimhan, AIP Conf. Proc. 34, 40 (1976).
[12] S. Anzai and K. Ozawa, J. Phys. Soc. Jpn. 24, 271 (1968).
[13] K. Kanematsu, J. Phys. Soc. Jpn. 17, 85 (1962).
[14] S. Fraga, J. Karwowski, and K. M. S. Saxena, *Handbook of Atomic Data* (Elsevier, Amsterdam, 1976), pp. 319 and 465.
[15] W. Jeitschko, Acta Crystallogr. B 31, 1187 (1975).
[16] I. Nebenzahl, Phys. Rev. 177, 1001 (1969).
[17] T_D strongly depends on composition (T_D^h = 380 K for $Mn_{0.92}NiGe$; 470 K for MnNiGe) (Ref. 9).
[19] T. Nagamiya, *Solid State Physics*, edited by F. Seitz, D. Turnbull, and H. Ehrenreich (Academic, New York, 1967), Vol. 20, p. 306.
[20] L. D. Landau and E. M. Lifshitz, *Statistical Physics* (Pergamon, London, 1962), Chap. 14.
[21] Equation (2) differs from Smolenskii's equation (1) (Ref. 7) in the choice of power series.
[22] In Refs. 3 and 4, the crossing nature between two second-order transition lines has been investigated in the case of [a]. The helimagnetic TiNiSi and the fictitious helimagnetic Ni_2In-type phases presumably correspond to the "intermediate phase" and phase III, respectively.